JOURNAL OF GEOPHYSICAL RESEARCH, VOL. 102, NO. D7, PAGES 8991–9001, APRIL 20, 1997

# Timescales for the stratospheric circulation derived from tracers

Timothy M. Hall and Darryn W. Waugh

Cooperative Research Centre for Southern Hemisphere Meteorology
Monash University, Clayton, Australia

**Abstract.** A class of atmospheric constituents used as tracers of stratospheric flow are chemically long-lived in comparison with timescales of interest and exhibit gradients due primarily to time-dependent mixing ratios at the tropopause. In general, the stratospheric transport properties derived from such tracers depend on the nature of their time variation. To explore the relationship between timescales associated with the propagation of tracer mixing ratio signals and bulk transport properties, we have used two three-dimensional chemical transport models to simulate the age spectrum (the distribution of transit times of mass present in air parcels) of the stratosphere. From the age spectrum the stratospheric response to any time-varying tropospheric forcing may be deduced. The modeled age spectra are broad, indicating a range of transit times present in air parcels, and asymmetric, so that the mean transit time, called the mean age, is much larger than the modal transit time. Furthermore, the phase lag time of an oscillating signal (e.g., the annual $CO_2$ cycle and lower stratospheric $H_2O$) and the mean age are not timescales characterizing the same transport property. Periodic signal phase lags do not represent "mean transit times" and, in general, cannot be readily related to bulk transport properties. However, if the age spectrum is peaked enough, as it appears to be in the lower tropical stratosphere, periodic signal phase lags approximate the modal time.

## 1. Introduction

In the last several years, satellite and aircraft campaigns have provided large quantities of high-quality observations of chemical constituents in the stratosphere. Analyses of many of these observations have been used to deduce far more detail of stratospheric transport mechanisms than was previously possible.

An example of considerable interest is the dynamical connection between the tropics and extratropics in the lower stratosphere. The Brewer-Dobson mass circulation of the stratosphere [*Brewer*, 1949] consists of entry into the stratosphere through the tropical tropopause and ascent through isentropes in the tropics, followed by poleward motion and descent in the extratropics, where ultimately, air reenters the troposphere. However, it is well established that through much of the year in the extratropical stratosphere an important additional mode of constituent transport occurs: quasi-isentropic mixing due to breaking planetary waves [e.g., *McIntyre*, 1992 and references therein]. If this rapid mixing were truly global (at least in an annually averaged sense), then the slope equilibrium limit of *Plumb and Ko* [1992], in which the mixing and the circulation cell are the dominant terms of the tracer continuity equation, would be a good approximation of the global shape of long-lived tracer mixing ratio surfaces. However, aircraft-observed variations in tracer-tracer correlation curves [*Murphy et al.*, 1993] and sharp gradients in satellite aerosol measurements [*Trepte and Hitchman*, 1992], among other observational studies, provide strong evidence that quasi-isentropic mixing is inhibited between the tropics and extratropics. In the opposite limit to global mixing, the "tropical pipe" of *Plumb* [1996], the tropics are completely isolated, and the only transport processes are ascent and entrainment to the extratropics. Clearly, the atmosphere lies between these two extremes, and a number of recent studies have worked to pin down more precisely the transport rate between the tropics and extratropics [*Boering et al.*, 1994, 1995; *Hintsa et al.*, 1994; *Volk et al.*, 1996; *Mote et al.*, 1995, 1996; *Avallone and Prather*, 1996; *Minschwaner et al.*, 1996].

One technique to deduce transport properties is the observation of the class of tracers whose source is in the troposphere, whose tropospheric abundance is approximately linearly time dependent, and whose photochemical lifetime in the lower stratosphere is at least a decade. Examples are the mean annual growth of $CO_2$ [*Bischof et al.*, 1985; *Schmidt and Khedim*, 1991; *Boering et al.*, 1994, 1996], some of the CFCs [*Pollock et al.*,



Paper number 96JD03713.
0148-0227/97/96JD-03713$09.00

1992] (although upward trends of CFC 11 and 12 have now slowed [*Elkins et al.*, 1993]), and $SF_6$ [*Rinsland et al.*, 1993; *Elkins et al.*, 1996; *Harnisch et al.*, 1996]. The mean gradients exhibited by these species are due primarily to the finite time required for new tracer-rich air to reach and spread through the stratosphere. The lag time of the stratospheric response from the tropospheric mixing ratio is the mean age of stratospheric air.

Most recently, a set of studies has looked at the propagation of oscillating tracer signals such as those of $CO_2$ and $H_2O$ [*Hintsa et al.*, 1994; *Boering et al.*, 1995, 1996; *Mote et al.*, 1995, 1996]. In the case of $CO_2$ the signal is forced at the surface by the seasonal variations of photosynthesis and respiration. For stratospheric water vapor the signal appears to be forced by the annual cycle in the tropical tropopause temperature, although the details remain poorly understood. In both cases the signal propagates into the stratosphere and is a significant part of the variability of mixing ratio up to about 10 mbar in the tropics and in the lowest part of the extratropical stratosphere. The rate of propagation and the amplitude variation represent information about stratospheric transport.

A major goal of this work is to illustrate that in general the phase lag of an oscillating signal and the lag of a linear trend are not timescales characterizing the same transport property. Although this point has been argued before in specific contexts [*Hall and Prather*, 1993; *Hall and Plumb*, 1994], it deserves further elaboration, given recent interest in propagating oscillating tracer signals. The conceptual tool that we believe makes the point most transparent is the age spectrum. Unfortunately, the age spectrum is not directly observable in the real atmosphere; we perform numerical experiments with two chemical transport models (CTMs) to determine the simulated age spectra and illustrate our discussion of tracer signal propagation.

In section 2 we define the age spectrum formally. Section 3 provides details of the models employed and the setup of the numerical experiments. We present the model results for the age spectra in section 4, showing the mean age and periodic signal propagation. We discuss interpretations of periodic signal phases in section 5, and we conclude in section 6.

## 2. Age Spectrum: Definitions

The age spectrum was presented in a trajectory calculation study of a model stratosphere by *Kida* [1983] and formally developed by *Hall and Plumb* [1994]. We present a brief general discussion here, referring readers to *Hall and Plumb* [1994] for more details.

The age spectrum is the function $G(t, \mathbf{x}, \mathbf{x}_0)$ such that $G(t, \mathbf{x}, \mathbf{x}_0)dt$ is the mass fraction of air at point $\mathbf{x}$ that had transit time between $t$ and $t+dt$ from point $\mathbf{x}_0$. Alternatively, with trajectory studies of irreducible fluid elements or particles in mind, the spectrum may be viewed as proportional to the number distribution of particles binned by their transit times from $\mathbf{x}$ to $\mathbf{x}_0$. The age spectrum is the Green's function of the assumed stationary continuity equation governing the atmospheric transport of a conserved tracer. Thus, if $n(t, \mathbf{x})$ is the mixing ratio of a conserved tracer in the stratosphere, and $n(t, \mathbf{x}_0)$ is the known tracer mixing ratio at at the surface, then

$$n(t, \mathbf{x}) = \int_0^t n(t - t', \mathbf{x}_0) G(t', \mathbf{x}, \mathbf{x}_0) dt' \qquad (1)$$

By expression (1) the age spectrum of any model (for example, a general circulation model (GCM) or a CTM) is produced directly by setting the surface mixing ratio boundary condition to a single spike (i.e., $n(t, \mathbf{x}_0) = \delta(t)$). The response is then simply $G(t, \mathbf{x}, \mathbf{x}_0)$. Once the age spectrum is known, the responses to all other time dependencies can be determined by the convolution summarized in expression (1).

Knowledge of $G(t, \mathbf{x}, \mathbf{x}_0)$ would help validate and quantify our understanding of transport mechanisms in the atmosphere. Although it seems unlikely that the age spectrum will be directly observed, characteristics of it can be deduced from tracer observations. For example, if the tropospheric time history is linear, as it is approximately for the constituents $SF_6$ and for $CO_2$ minus its annual cycle, then the first moment of the spectrum (the mean of the transit time distribution),

$$\Gamma(\mathbf{x}, \mathbf{x}_0) = \int_0^\infty t\, G(t, \mathbf{x}, \mathbf{x}_0) dt \qquad (2)$$

is equal to the stratospheric lag time, i.e., $n(t, \mathbf{x}) = n(t - \Gamma, \mathbf{x}_0)$. $\Gamma(\mathbf{x}, \mathbf{x}_0)$ is the mean age at $\mathbf{x}$ with repect to $\mathbf{x}_0$. The response to a sinusoidal time history $e^{i\omega t}$ has the amplitude and phase

$$A(\omega) e^{-i\phi(\omega)} = \int_0^\infty e^{-i\omega t} G(t, \mathbf{x}, \mathbf{x}_0) dt \qquad (3)$$

Thus the response yields a frequency component of the age spectrum. The mean age $\Gamma$, the phase lag time of periodic signals $\tau_\omega$, and other timescales discussed here are summarized in Table 1.

The age spectrum is a particularly useful conceptual tool in the stratosphere, because if the source is in the troposphere, the stratospheric response is only weakly dependent on its specific location. For example, $CO_2$ has a geographically varied pattern of sources and sinks, and thus, in principle, the atmospheric response to an impulse with a $CO_2$-like surface distribution is an average of the age spectra at each surface point weighted by the $CO_2$ mixing ratio at the point (see appendix A of *Plumb and McConalogue* [1988] for a more formal discussion). However, the atmospheric response to $CO_2$ loses zonal asymmetry rapidly with height, and in the upper troposphere and stratosphere, $CO_2$ is essentially independent of the longitudal structure of source and sink [*Heimann et al.*, 1989]. This fact implies that the

**Table 1.** Timescale Definitions

| Name | Symbol | Expression | Description |
|---|---|---|---|
| mean age | $\Gamma(\mathbf{x})$ | $\int_0^\infty tG(\mathbf{x},t)dt$ | mean of transit time distribution |
| spectral width | $\Delta(\mathbf{x})$ | $[\frac{1}{2}\int_0^\infty (t-\Gamma(\mathbf{x}))^2 G(\mathbf{x},t)dt]^{1/2}$ | measure of width of transit time distribution |
| modal time | $\tau_M(\mathbf{x})$ | $t$ such that $\partial G(\mathbf{x},t)/\partial t = 0$ | mode of the transit time distribution |
| phase lag time | $\tau_\omega(\mathbf{x})$ | $-\frac{1}{\omega}\arg[\int_0^\infty e^{-i\omega t}G(\mathbf{x},t)dt]$ | propagation time of periodic signal of frequency $\omega$ |

source-weighted average of the age spectrum around a latitude circle is approximately equal to the zonal-mean age spectra times the zonal-mean surface $CO_2$ mixing ratio. Here, we consider only zonal-mean spectra and sources; the labels $\mathbf{x}$ and $\mathbf{x}_0$ in the definitions above refer to points in the latitude-height plane. Furthermore, because most air enters the stratosphere in the tropics, the stratospheric age spectrum is also only weakly dependent on the latitude of the surface source. The tropical tropopause acts as an effective point source (in a zonal-mean sense) for the stratosphere.

## 3. Three-Dimensional Transport Simulations

### 3.1. Description of Models

To illustrate the role of the age spectrum in determining the stratospheric response to tracer signals forced by various time dependencies, we have performed numerical transport experiments with wind data computed by two GCMs: (1) the National Center for Atmospheric Research Middle Atmosphere Community Climate Model 2 (NCAR MACCM2) [*Boville*, 1995] and (2) the Goddard Institute for Space Studies' Global Climate Middle Atmosphere Model (GISS GCMAM) [*Rind et al.*, 1988]. Our experiments were run with "off-line" CTMs. The CTMs employ archived wind histories from the MACCM2 and GCMAM to advect tracer through the model atmosphere. For the experiments reported here, no photochemical calculations were required. We briefly summarize the two CTMs.

**Rasch-Williamson CTM driven by MACCM2.** The CTM of Phil Rasch and Dave Williamson [*Rasch et al.*, 1994] has a semi-Lagrangian transport scheme [*Williamson and Rasch*, 1989; *Rasch and Williamson*, 1990], which preserves shapes of tracer distributions and mimimizes numerical diffusion. The scheme is not implicitly mass conservative; a "mass fixer" may be employed after advection to keep global tracer mass constant. We drive the CTM with daily averaged MACCM2 wind components in the zonal, meridional, and vertical directions. The CTM grid is selected to match the GCM gridding of the wind data, which for the MACCM2 is 128 × 64 longitude by latitude points giving an approximate horizontal resolution of 2.8° × 2.8°. There are 44 vertical levels from the surface to about 80 km. Of those, 28 are at fixed pressure levels above 16 km; the vertical resolution in the lower stratosphere is approximately 1.4 km. No explicit diffusion or parameterized sub-grid scale mixing of tracer is included.

**Prather CTM driven by GISS GCMAM.** The CTM of Michael Prather [*Prather et al.*, 1987] uses a quadratic upstream transport scheme [*Prather*, 1986] that is mass conservative and exhibits low numerical diffusion. Here the model is driven by 8-hourly-averaged GCMAM wind data. The CTM grid matches the GCM grid: in the horizontal, 36 longitudes and 24 latitudes, corresponding to a resolution of 10.0° × 7.8° longitude by latitude, and in the vertical, 21 levels from the surface to about 85 km. Twelve of these levels are in the stratosphere at fixed pressure. In the transport simulations the coarse resolution is partly compensated by the sub-grid scale quadratic tracer distribution employed in the transport scheme. We use this information to diagnose tracer mixing ratios at a finer scale in the vertical than the fundamental grid. No explicit tracer diffusion or mixing is included in the stratosphere. The CTM simulates the tracer mixing effect of convection in the troposphere with a scheme based on monthly convection statistics archived from the GISS GCM.

From here on we use "CCM2" to refer to the Rasch-Williamson CTM driven by MACCM2 winds data and "GISS" to the Prather CTM driven by GISS wind data.

### 3.2. Experiment Details

The age spectrum with respect to a surface point $\mathbf{x}_0$ is the model response to a boundary condition at $\mathbf{x}_0$ having a delta function time dependence. As we noted above, the stratospheric response is not sensitive to the position or extent of the boundary condition region. For these runs the region consists of a zonal band centered on the equator of latitudinal extent two grid boxes (7.8°S to 7.8°N for GISS and 2.8°S to 2.8°N for CCM2). In both models the region extends vertically over the lowest three model levels, corresponding to about 1 km for GISS and 0.75 km for CCM2. To approximate the delta function time dependence the mixing ratio is set to an arbitray nonzero value for the first time step and is subsequently held at zero. From a start date of October 1 we ran GISS and CCM2 for 20 model years, saving instantaneous three-dimensional mixing ratio fields every 15 days. Note that in each run a single year of wind data is used, and thus no interannual transport variability is modeled.

## 4. Modeled Age Spectra

The age spectrum allows us to understand the model response to various time-dependent forcings in a unified fashion. In the process we can gain insight into observed tracer signals in the real atmosphere and how they relate to atmospheric transport timescales. We first focus on the mean age, and then the shape of the spectra and propagating signals. We present zonally averaged quantities; timescales referred to in the discussion are understood to have been averaged about a latitude circle.

### 4.1. Zonally Averaged Mean Age

Figure 1 shows the zonally averaged mean age $\Gamma$ contoured in years for CCM2 and GISS. The values are determined from the age spectra by expression (2). The GISS age was also shown by *Hall and Prather* [1993] and *Hall and Plumb* [1994]. In all figures the vertical coordinate is pressure altitude defined by $z^* = 16 \log(1000/p)$, where $p$ is in millibars and $z^*$ is in kilometers.

Both models show $\Gamma$ contour shapes generally characteristic of all long-lived tracers: an upward bulge in the tropics and a downward slope to the poles dictated by the balance between the slope steepening of the Brewer-Dobson mass circulation and slope flattening of the quasi-isentropic mixing in middle latitudes. Lower stratospheric tropical air is youngest, being closest to the point of injection of fresh tropospheric air, while upper atmospheric air at high latitudes is the oldest. Note that although gradients of $\Gamma$ are nearly independent of the location of the tropospheric source, the magnitude varies slightly. Using the GISS model, *Hall and Plumb* [1994] found a uniform increase of 0.7 years in $\Gamma$ in the stratosphere when the source was shifted from 3.9°S to 43.1°N. The magnitude of the shift is likely to be model dependent, but the observation that source shifts introduce only uniform stratospheric age offsets should be general.

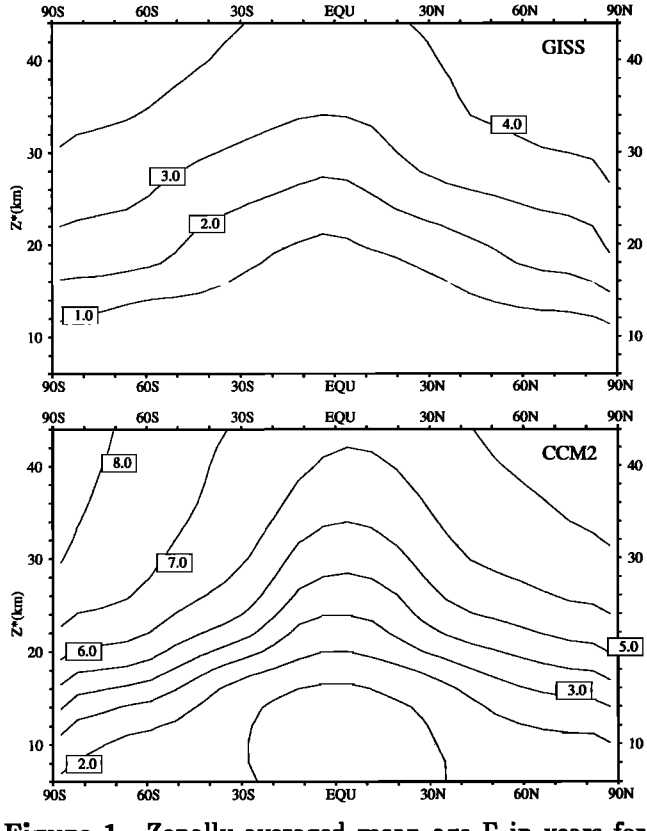


**Figure 1.** Zonally averaged mean age $\Gamma$ in years for (top) GISS and (bottom) CCM2.

**There are large differences between the two models in both the vertical and horizontal gradients. The CCM2 $\Gamma$ distribution is more realistic, matching well $\Gamma$ determined from measurements of $SF_6$ by both aircraft [*Elkins et al.*, 1996], which show up to 3-year age variations from equator to high latitudes at constant altitude, and balloons [*Harnisch et al.*, 1996], which show values up to 10 years in the polar vortex and 6 years at midlatitudes in the lower stratosphere. (Detailed comparisons of CCM2 age to observations are made by D. Waugh et al., Three-dimensional simulations of long-lived tracers using winds from MACCM2, submitted to *J. Geophys. Res.*, (1996)). Vertical gradients of $\Gamma$ in the lower GISS stratosphere are known to be too weak [*Hall and Prather*, 1993], likely a consequence of the model's coarse resolution. For the purposes of this study these quantitive model differences might be considered a strength: two very different simulations support the same conclusions, providing more generality to the argument.**

The modeled $\Gamma$ distributions are both very different from the distribution *Rosenlof* [1995] determined by advecting air parcels with an estimate of the stratospheric residual circulation. The CCM2 and GISS simulations include the transport effects of quasi-isentropic mixing as well as the residual circulation. The quasi-isentropic mixing significantly reduces the slopes of the $\Gamma$ contours and enhances the tropical $\Gamma$ values in comparison with transit times of parcels transported by the residual circulation alone. This mixing must be included for realistic mean age distributions.

### 4.2. Age Spectra Shape

Figure 2 shows the zonal-mean age spectra for GISS at four pressure altitudes in the lower stratosphere in the tropics and high latitudes. Also indicated are the mean age $\Gamma$ and the spectral width $\Delta$ (dotted lines; see the appendix for the definition of the spectral width) and the phase lag time $\tau_\omega$ from the source of a sinusoid of period 1 year (dashed line; see section 4.3). Figure 3 is an identical plot for the CCM2 model.

The asymmetry of the age spectra is a striking feature in both models: the spectra have "long tails." Consequently, $\Gamma$ is much greater than the time of the spectral peak throughout the model stratospheres. We refer

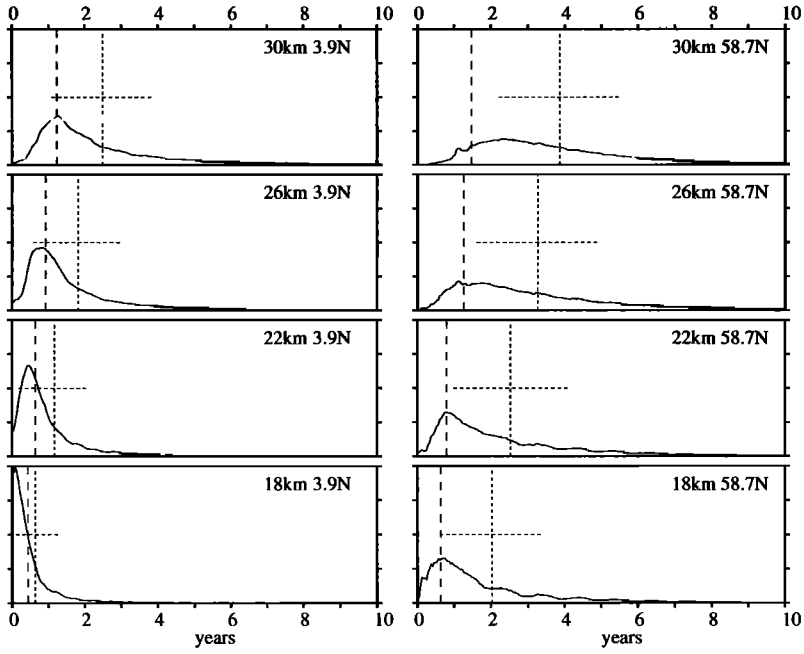


**Figure 2.** Zonal mean age spectra of GISS at the latitudes 3.9°N and 58.7°N and pressure altitudes 18 km, 22 km, 26 km, and 30 km as labeled. The horizontal axis is labeled in years. The dotted vertical line indicates the mean age $\Gamma$, while the length of the dotted horizontal line represents twice the spectral width ($2\Delta$). The dashed vertical line is the phase lag time $\tau_\omega$ of the response to a sinusoidal annual cycle (phase is defined as zero at the surface source).

to the spectral peak time as the "modal" transit time; if the spectral peak is at time $\tau_M$, then the interval $\tau_M d\tau$ encompasses the transit time of more mass than any other equal sized interval. $\Gamma$, on the other hand, is a transport diagnostic strongly influenced by small amounts of mass requiring transit times much longer than $\tau_M$, and hence $\Gamma >> \tau_M$. The time at which half the air is younger and half older (the median time) lies between $\tau_M$ and $\Gamma$.

At the tropical tropopause the spectra are most like the delta function source: $\tau_M$ and $\Gamma$ are smallest and closest to each other. In the stratosphere, however, air

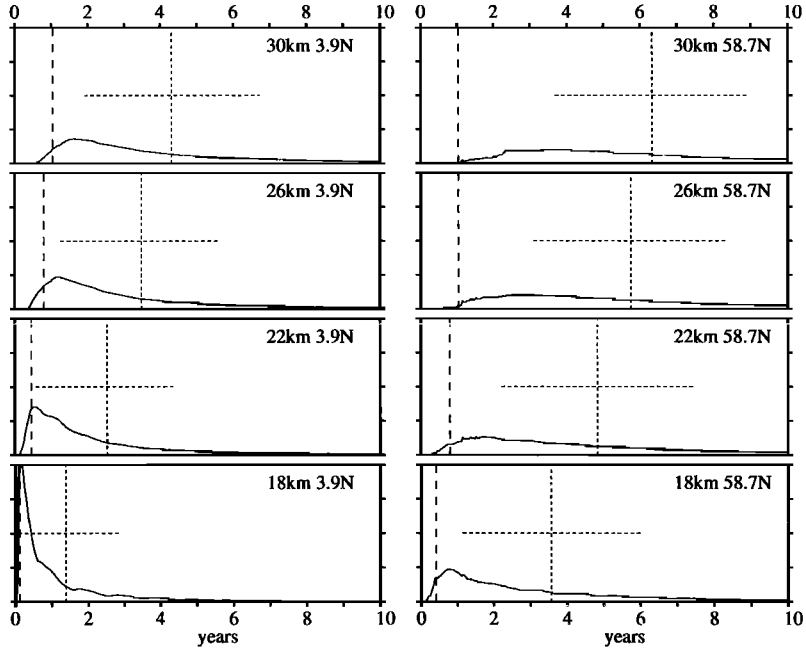


**Figure 3.** As in Figure 2, but for the CCM2 model. For the sake of comparison, all CCM2 results have been interpolated to the GISS latitude and height grid for plotting.

masses of differing transit times mix, causing a broadening of the age spectrum. Above the tropopause, $\tau_M$ increases. In addition, the tail region becomes more prominent, increasing the difference between $\Gamma$ and $\tau_M$. These two quantities are shown in profile in Figure 4 .

At constant pressure altitude, extratropical spectra have greater $\Gamma$ and greater $\tau_M$ and are broader (larger $\Delta$) than those in the tropics. Figure 5 displays the latitudinal dependence of the modal time, phase lag, and mean age at 20 km.

### 4.3. Propagation of a Repeating Signal

The phase lag time $\tau_\omega$ in the stratosphere of an annually periodic tracer forcing, like $\tau_M$, is in both models everywhere significantly less than $\Gamma$. We simulate the stratospheric response to a tropospheric time history by convolving the age spectra with a sinusoid of 1 year period, producing a phase and amplitude given by expression (3). Figures 2 and 3 show the phase lag for GISS and CCM2 as a vertical dashed line superposed on the age spectra. The phase lags are also plotted versus height at 3.9°N in Figure 4 and versus latitude at

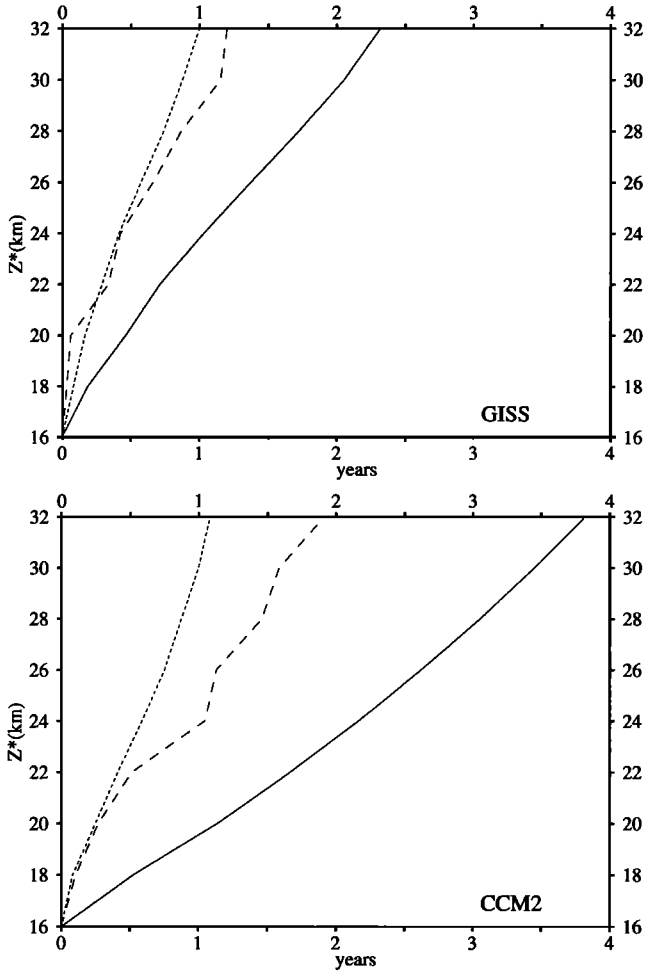


**Figure 4.** Vertical profiles at 3.9°N of the $\Gamma$ (solid line), $\tau_M$ (dashed line), and $\tau_\omega$ (dotted line) for $\omega = 2\pi/1$ year. (top) GISS. (bottom) CCM2.

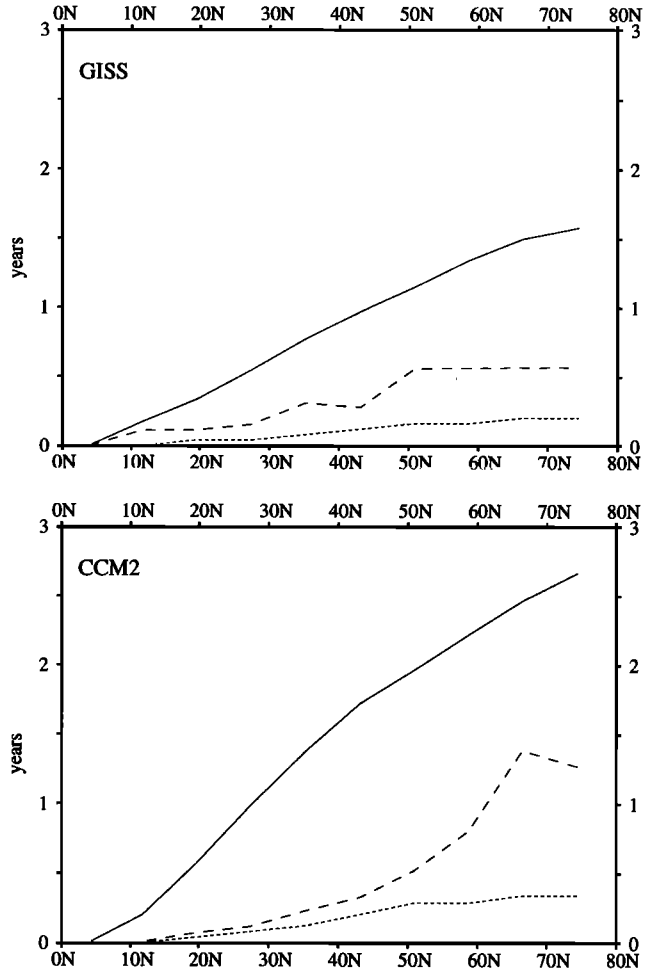


**Figure 5.** Latitudinal profiles at 20 km of $\Gamma$ (solid line), $\tau_M$ (dashed line), and $\tau_\omega$ (dotted line). (top) GISS. (bottom) CCM2.

20 km in Figure 5 as a dotted line. The bottom panel of Figure 6 displays the peak-to-peak amplitude versus altitude at 3.9°N of the two models. The amplitudes are scaled to have unit magnitude at 18 km.

A striking feature of $\tau_\omega$ (Figure 4) is its good match with $\tau_M$ in the lower tropical stratosphere of the models. This agreement holds to above 32 km for GISS. For CCM2, with the more realistic spatial $\Gamma$ distribution, it breaks down above 22 km. As a function of latitude, $\tau_\omega \approx \tau_M$ from the equator to midlatitudes, although there is little variation of either in this region, particularly for GISS. At higher latitudes, $\tau_\omega < \tau_M$.

In both models the amplitude attenuates rapidly with height. As age spectra broaden with altitude, progressively more cycles of the periodic forcing are averaged (see expression (3)). By 26 km in the tropics the model signal amplitudes have decreased to about 0.10 (GISS) and 0.05 (CCM2) of their tropopause magnitudes.

## 5. Interpreting the Phase Propagation

The model results show that the response to an oscillating signal is quite different from the response to

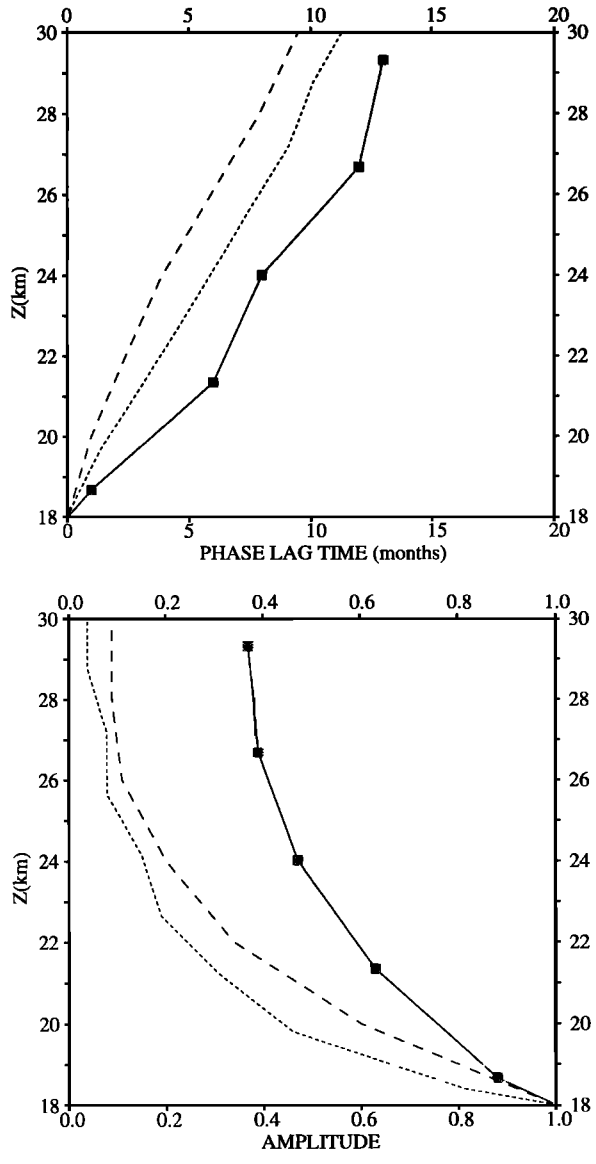


**Figure 6.** (top) Vertical profiles at 3.9°N of $\tau_\omega$ in CCM2 (dotted) and GISS (dashed). The solid line and symbols are $\tau_\omega$ of a harmonic fit to the 4 year HALOE $H_2O$+2$CH_4$ time series (W. Randel et al., Seasonal cycles and interannual variability in stratospheric $CH_4$ and $H_2O$ observed in UARS HALOE data, submitted to *J. Atmos. Sci*, (1996)). Each profile is referenced to zero at 18 km. (bottom) Three corresponding vertical profiles of the peak-to-peak amplitude (normalized to unity at 18 km).

a linear increase, which yields $\Gamma$. Regardless of the shape of the age spectrum, $\Gamma(\mathbf{x})$ is the mean transit time from the troposphere of all the air at x. In general, no such simple relationship holds between mean transit time and stratospheric tracer signals for nonlinear tropospheric trends [*Hall and Plumb*, 1994]. For periodic tracer signals at the tropopause, whether $\tau_\omega$ can be related to bulk transport properties depends on the age spectral shape compared to the period of forcing. Thus, unlike the response of a linearly increasing tracer, interpreting periodic time dependencies requires some a priori knowledge of, or assumptions about, the transport itself.

One possible assumption is the idealized stratosphere described by the "tropical pipe" model [*Plumb*, 1996], in which there is no mixing of midlatitude air into the tropics. If we further assume that the tropical ascent rate is a constant and uniform $w$, then a pulse of air entering the pipe through the tropopause rises at $w$, preserving its identity. In such a model the tropical age spectrum is a delta function. $\Gamma$ and $\tau_\omega$ are identical, both given by the time lag of the propagating pulse, as can be seen by substituting $G(\mathbf{x},t) = \delta(t - |\mathbf{x}|/w)$ in expressions (2) and (3).

The real atmosphere falls short of being completely in the tropical pipe limit [*Volk et al.*, 1996; *Mote et al.*, 1996; *Avallone and Prather*, 1996; *Minschwaner et al.*, 1996]. Midlatitude air mixes into the tropical plume, and the ascent rate within the plume is not perfectly uniform. Both effects broaden the age spectra away from a delta function; a range of transit times from the tropical tropopause is present. Even in the relatively isolated tropical stratosphere, over seasons to years, air masses do not retain their identity, but instead mix with other masses of differing tracer properties and transit times. On such time spans, "air parcel" or "air mass" is only a conceptual tool operating in the point-like limit of zero mass. Thus transport timescales deduced from radiatively determined vertical velocities in the tropics [e.g., *Weinstock et al.*, 1995] should not be associated with a time since any particular air mass entered the stratosphere, as no such single transit time exists.

How, then, can $\tau_\omega$ be interpreted? A weaker assumption than complete tropical isolation is that of enough isolation for the age spectrum to retain its delta function property of picking out the phase of an annual cycle. This occurs in regions of the two model atmospheres (Figures 2 and 3). In the lower tropical stratosphere of the models the spectra are sharply peaked with only a low-amplitude tail. The long tail draws $\Gamma$ away from $\tau_M$. However, it adds little to the response of the oscillating forcing, as several cycles are averaged. Only the peak region will contribute significantly to the response. If this region is narrow enough in comparison with the period of the forcing, then $\tau_\omega \approx \tau_M$.

If the age spectra in the real atmosphere broadened more rapidly with height than the model spectra, the connection between $\tau_M$ and $\tau_\omega$ would be less robust. However, more rapid broadening would also mean more rapid attenuation of the amplitude of periodic tracer signals. In fact, the opposite is true: the atmosphere attenuates the amplitude significantly less strongly than either model, implying narrower spectra than the models predict. This finding can be seen in Figure 6, which in addition to the model profiles, also shows the amplitude profile of a two-component (annual and semiannual) harmonic fit to the 4-year time series of the Halogen Occultation Experiment (HALOE) $H_2O$+2$CH_4$, as calculated by W. Randel et al. (Seasonal cycles and in-

terannual variability in stratospheric $CH_4$ and $H_2O$ observed in UARS HALOE data, submitted to *J. Atmos. Sci*, (1996)). There is interannual variability in the observed amplitude attenuation: for example, following the propagation of individual annual cycles reveals a range of 0.45 to 0.70 at 21.3 km (46.3 mbar). Nevertheless, it is clear that both CCM2 and GISS significantly underestimate the amplitude of an annual cycle (and also underestimate $\tau_\omega$, as can be seen in the top panel of Figure 6). Observations of the $CO_2$ annual cycle in the tropics are consistent with HALOE, showing a 0.8 fractional amplitude at 435°K ($\approx$ 19 km) in comparison with the tropopause value [*Boering et al.*, 1996].

We conclude that in the lower tropical stratosphere, for $\omega = 2\pi/1$ year, $\tau_\omega$ is a measure of $\tau_M$, the transit time taken by more mass than any other. *Mote et al.* [1995] have shown that the observed phase speed of the $H_2O+2CH_4$ annual cycle also approximately tracks the ascent of the stratosphere's diabatic mass circulation.

The situation at midlatitudes is less clear. In the models, $\tau_\omega \approx \tau_M$ at lower latitudes where there is little variation in either (Figure 5). At higher latitudes, $\tau_\omega < \tau_M$; the spectra are wide enough for several cycles of oscillation to contribute with comparable magnitudes to the averaging, resulting in low amplitudes and residual phase that is difficult to interpret.

Another subtlety of interpreting $\tau_\omega$ in the stratosphere may occur if the time dependency of the signal at the tropical tropopause is nonsinusoidal. The width and asymmetry of the age spectrum imply a dependence of the response amplitude and phase on the frequency of forcing $\omega$. Higher-frequency components attenuate more rapidly and propagate more quickly. Thus, if a time-dependent forcing has a range of frequency components, its shape will change as it propagates; it will evolve so that its time signal away from the source is closer to the basest mode. The phase change of the minimum extrema of a cycle is not, in general, equal to that of the maximum, as the duration from minimum to maximum may vary.

Although $\tau_\omega$ is not everywhere readily related to bulk transport properties, one general observation is that it is everywhere less than $\Gamma$. We argue in the appendix that this result is true for any age spectrum having a long tail. Timescales inferred from phases of periodic signals in the stratosphere [*Boering et al.*, 1994; *Mote et al.*, 1995] do not, in general, equal the mean transit time, or mean age $\Gamma$, from the tropopause. This difference has been seen in the lower tropical stratosphere upon comparing the phase lag of the $CO_2$ annual cycle to $\Gamma$ deduced from $SF_6$ (K. Boering, personal communications, 1996).

## 6. Conclusions

We have used two three-dimensional chemical transport models to simulate the age spectrum (the distribution of transit times of mass present in stratospheric air parcels). The age spectra allow us to draw general conclusions about the how the stratosphere responds to different time dependencies of long-lived tracer mixing ratio at the tropopause. The modeled age spectra are broad, indicating that many transit times are represented in an air parcel: air parcels are not transported intact over seasons and years. The age spectra are also asymmetric, so that the mean of the transit time distribution (the mean age $\Gamma$) is much larger than the mode $\tau_M$ of the distribution.

The shape of the modeled age spectrum says several things about the interpretation of observed variations in long-lived tracers: (1) The phase lag time $\tau_\omega$ for annually repeating signals is much less than the mean age $\Gamma$; in other words, measuring the propagation of a periodic signal does not directly yield a "mean transit time." (2) It is not clear that $\tau_\omega$ is, in general, related to a bulk transport property. (3) However, if the age spectrum is peaked enough, as it appears to be in the lower tropical stratosphere, $\tau_\omega \approx \tau_M$.

Knowing the age spectrum of the real atmosphere would help quantify our understanding of transport mechanisms. However, at present, there is no direct way to observe the stratospheric age spectrum; such observation would require an instantaneous release of conserved tracer at or below the tropopause with a mixing ratio much larger than background levels. Nevertheless, aspects of the spectral shape can be inferred, given observations of appropriate tracers. While the stratospheric response to a quasi-linearly varying tracer such as $SF_6$ depends only on $\Gamma$, the response to exponentially increasing tracers depends also on the width $\Delta$ of the age spectrum (see equations (10) through (12) of *Hall and Plumb* [1994]). The trace gas HCFC-142b ($CH_3CF_2Cl$) is long-lived in the stratosphere and has been undergoing rapid enough exponential increase in the troposphere [*Oram et al.*, 1995] so that it might be possible to use measurement of its mixing ratio, in combination with determinations of $\Gamma$, to deduce $\Delta$. Furthermore, $\tau_M$ may be approximately determined, at least in the tropics, from the propagation of $CO_2$ or $H_2O$ annual cycles. Thus, although the age spectrum is unlikely to be directly observed, knowledge of $\Gamma$, $\tau_M$, and possibly $\Delta$ will characterize important aspects of its shape.

Balloon measurements of $SF_6$ and $CO_2$ through the lower and middle tropical stratosphere as part of the Observations from the Middle Stratosphere (OMS) campaign are presently being made that will clarify these age spectral timescales and thus will provide valuable tests of model transport. A comparison of modeled and observed $\Gamma$ cannot by itself completely validate model transport, as a realistic mean for the modeled age spectrum says nothing about the realism of the transport's dispersion. Such dispersion information is contained in the shape of the age spectrum. However, if, in addition to $\Gamma$, $\tau_\omega$ and the annual cycle amplitude are deduced from observations, the model's age spectral shape may

be stringently tested, at least in the lower and middle tropical stratosphere and the extratropical lower stratosphere where tracer annual cycles are large enough to observe.

The CCM2 mean age distribution has significantly stronger gradients and reaches values older than those of GISS, features confirmed by aircraft and balloon observations of $SF_6$ [*Elkins et al.*, 1996; *Harnisch et al.*, 1996]. (Detailed comparisons of CCM2 calculations and $SF_6$ observations are made by D. Waugh et al., Three-dimensional simulations of long-lived tracers using winds from MACCM2, submitted to *J. Geophys. Res.*, (1996).) Both models, however, underestimate the annual cycle amplitude and $\tau_\omega$ through the tropical lower and middle stratosphere in comparison with HALOE $H_2O+2CH_4$ observations. Either the models do not isolate the tropics enough, or they have too strong vertical diffusion, or both.

Finally, we note that although the mean age is a useful diagnostic of stratospheric transport, it is not necessarily a critical model parameter determining the simulation realism of many chemically active species. For a constituent near photochemical equilibrium, transport timescales are not directly relevant. However, even for constituents with intermediate chemical lifetimes, $\Gamma$ may not be the most influential timescale. $\Gamma$ is quite sensitive to the tail region of the age spectrum, while a photochemically active constituent is not, if its chemical lifetime is shorter than the transit times of the tail region. For example, at 30 km in the tropics the chemical lifetime of $N_2O$ is about a year; transit times from the troposphere to 30 km longer than 1 year will influence $\Gamma$ but will not affect the $N_2O$ mixing ratio significantly. For $O_3$, inaccuracies in the tail region of the spectrum will be still less important. On the other hand, accurate simulation of $\tau_M$ may be quite important, as the species are closer to conserved on this shorter timescale.

## Appendix: $\tau_\omega$ Compared to $\Gamma$

Consider the response $n(\mathbf{x},t)$ to a sinusoidal forcing $e^{i\omega t}$ at $\mathbf{x}=\mathbf{0}$. By expression (1),

$$n(\mathbf{x},t) = e^{i\omega t}\int_0^\infty e^{-i\omega t'}G(\mathbf{x},t')dt' \qquad \text{(A1)}$$

The integral can be expanded in moments of the age spectrum, producing to order $\omega^3$

$$n(\mathbf{x},t) \sim e^{i\omega t}(1-\omega^2\Delta^2(\mathbf{x}))e^{-i\omega[\Gamma(\mathbf{x})-\omega^2\Sigma^3(\mathbf{x})]} \qquad \text{(A2)}$$

where $\Gamma(\mathbf{x})$ is the first moment given by expression (2), $\Delta(\mathbf{x})$ and $\Sigma(\mathbf{x})$ are the second and third moments of the age spectrum,

$$\Delta^2(\mathbf{x}) = \frac{1}{2}\int_0^\infty (t-\Gamma(\mathbf{x}))^2 G(\mathbf{x},t)dt \qquad \text{(A3)}$$

$$\Sigma^3(\mathbf{x}) = \frac{1}{6}\int_0^\infty (t-\Gamma(\mathbf{x}))^3 G(\mathbf{x},t)dt \qquad \text{(A4)}$$

and $O(\omega^4)$ indicates the presence of terms quartic and higher in the forcing frequency $\omega$. This expansion converges in the low-frequency limit, i.e., when the period of forcing is larger than the characteristic dimensions (moments) of the spectrum. Thus, in this limit the phase lag of the response, $\tau_\omega(\mathbf{x})$, is

$$\begin{aligned}\tau_\omega(\mathbf{x}) &= -\frac{1}{\omega}\arg\Big[\int_0^\infty e^{-i\omega t}G(\mathbf{x},t)dt\Big] \\ &\sim \Gamma(\mathbf{x}) - \omega^2\Sigma^3(\mathbf{x}) \qquad \text{(A5)}\end{aligned}$$

Thus it is the asymmetry of the age spectrum, as summarized by $\Sigma(\mathbf{x})$, that is responsible for the difference between phase lag and mean age. The essence of this asymmetry is most apparent to us in the descriptive limit of irreducible fluid elements ("particles") of vanishing mass, undergoing statistical motion. Diffusive aspects to the mass transport guarantee that there are paths for particles of arbitrarily long duration connecting some point $\mathbf{x}_0$ to some other point $\mathbf{x}$. The probability of a particle taking a particular long duration path may be vanishingly small, but not zero. Thus whatever the most common transit time from $\mathbf{x}_0$ to $\mathbf{x}$ (the modal time $\tau_M$), there are arbitrarily longer times taken by at least some particles. On the other hand, times shorter than $\tau_M$ must still be greater than zero; hence the positive asymmetry ($\Sigma(\mathbf{x}) > 0$). By (A5), then, $\tau_\omega < \Gamma$ for small $\omega$.

We are not able to be general away from the low-frequency regime. Instead we look at specific age spectra. *Hall and Plumb* [1994] found the age spectrum for a one-dimensional mass weighted diffusion equation with uniform scale height and diffusion coefficient and gave an expression for the response to an oscillating source. Combining their equation (28) for the phase and their (22) for the mean age gives

$$\frac{\tau_\omega}{\Gamma} = \frac{2}{\omega\tau_K}(1+\omega^2\tau_K^2)^{1/4}\sin\big(\frac{1}{2}\tan(\omega\tau_K)\big) \qquad \text{(A6)}$$

where $\tau_K = 4H^2/K$ is the characteristic time to diffuse two scale heights $H$, given a uniform diffusivity $K$. This function, always less than one, is plotted in Figure 7 for a time constant $\tau_K = 2$ years. (This $\tau_K$ corresponds to $K = 3\ \mathrm{m^2 s^{-1}}$, a somewhat arbitrary value selected to make the resulting age spectra look roughly like the zonally and latitudinally averaged GISS spectra [*Hall and Plumb*, 1994]. In this context, $K$ models a global one-dimensional transfer coefficient and is not representative of $K_{zz}$ in the atmosphere.) Also plotted is the $\tau_\omega/\Gamma$ ratio from CCM2 for a range of frequencies.

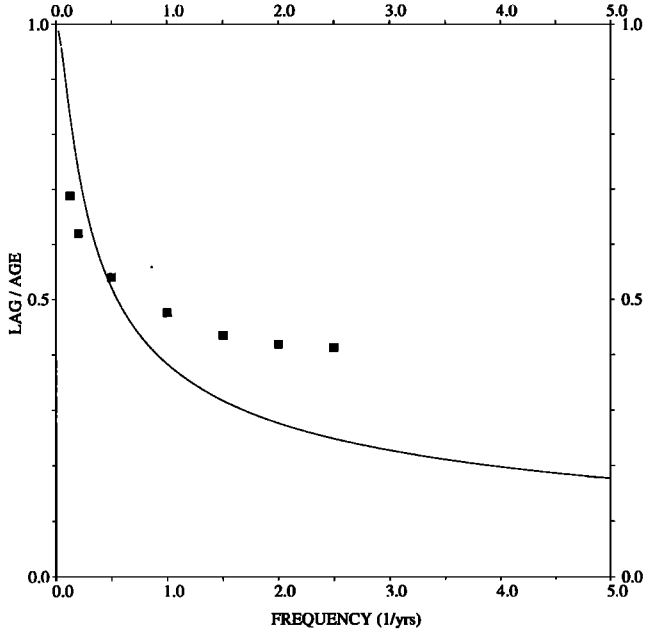


**Figure 7.** The $\tau_\omega$ values versus the frequency of forcing $\omega$. The vertical coordinate is $\tau_\omega/\Gamma$. The solid line is for the analytic result for the one-dimensional mass weighted diffusion equation (time constant for diffusion over two scale heights $\tau_K = 2$ years), and the symbols are from the CCM2 model at 3.9°N and 22 km.

spectra (one-dimensional diffusion and CCM2 model) we conclude that $\tau_\omega < \Gamma$ for all $\omega$.

**Acknowledgments.** We thank Michael Prather for his ideas that in part motivated this work and for insightful comments on the manuscript. Phil Rasch provided and helped us with the Rasch-Williamson transport model. We also thank Kristie Boering for discussing her aircraft data before publication, Bill Randel for providing us his harmonic fits of HALOE $H_2O$+2$CH_4$ data, Ming Luo for discussing HALOE observations, and Dave Fahey and Alan Plumb for helpful comments of the manuscript. This research was supported through the Australian Government Cooperative Research Centre Program.

## References

Avallone, L. M., and M. J. Prather, Photochemical evolution of ozone in the lower tropical stratosphere, *J. Geophys. Res.*, *101*, 1457–1461, 1996.

Bischof, W., R. Borchers, P. Fabian, and B. C. Kruger, Increased concentration and vertical distribution of carbon dioxide in the stratosphere, *Nature*, *316*, 708–710, 1985.

Boering, K. A., B. C. Daube, S. C. Wofsey, M. Loewenstein, J. R. Podolske, and E. R. Keim, Tracer-tracer relationships and lower stratospheric dynamics: $CO_2$ and $N_2O$ correlations during SPADE, *Geophys. Res. Lett.*, *21*, 2567–2570, 1994.

Boering, K. A., et al., Measurements of stratospheric carbon dioxide and water vapor at northern midlatitudes: Implications for troposphere-to-stratosphere transport, *Geophys. Res. Lett.*, *22*, 2737–2740, 1995.

Boering, K. A., S. C. Wofsy, B. C. Daube, H. R. Schneider, M. Loewenstein, and J. R. Podolske, Sratospheric transport rates and mean age distribution derived from observations of atmospheric $CO_2$ and $N_2O$, *Science*, *274*, 1340–1343, 1996.

Boville, B. A., Middle atmosphere version of the CCM2 (MACCM2): Annual cycle and interannual variability, *J. Geophys. Res.*, *100*, 9017–9039, 1995.

Brewer, A. W., Evidence for a world circulation provided by the measurements of helium and water vapor distribution in the stratosphere, *Q. J. R. Meteorol. Soc.*, *75*, 351–363, 1949.

Elkins, J. W., T. M. Thompson, T. H. Swanson, J. H. Butler, B. D. Hall, S. O. Cummings, D. A. Fisher, and A. G. Raffo, Decrease in the growth rates of atmospheric chlorofluorocarbons 11 and 12, *Nature*, *364*, 780–783, 1993.

Elkins, J. W., et al., Airborne gas chromatograph for in situ measurements of long-lived species in the upper troposphere and lower stratosphere, *Geophys. Res. Lett.*, *23*, 347–350, 1996.

Hall, T. M., and R. A. Plumb, Age as a diagnostic of stratospheric transport, *J. Geophys. Res.*, *99*, 1059–1070, 1994.

Hall, T. M., and M. J. Prather, Simulations of the trend and annual cycle in stratospheric $CO_2$, *J. Geophys. Res.*, *98*, 10,573–10,581, 1993.

Harnisch, J., R. Borchers, P. Fabian, and M. Maiss, Tropospheric trends for $CF_4$ and $C_2F_6$ since 1982 derived from $SF_6$ dated stratospheric air, *Geophys. Res. Lett.*, *23*, 1099–1102, 1996.

Heimann, M., C. D. Keeling, and C. J. Tucker, A three-dimensional model of atmospheric $CO_2$ transport based on observed winds, 3, Seasonal cycle and synoptic time scale variations, in *Aspects of Climate Variability in the Pacific and the Western Americas, Geophys. Monogr.*, 55, edited by D. H. Peterson, pp. 277–303, AGU, Washington, D. C., 1989.

Hintsa, E. J., E. M. Weinstock, A. E. Dessler, J. G. Anderson, M. Lowenstein, and J. R. Podolske, SPADE $H_2O$ measurements and the seasonal cycle of stratospheric water vapor, *Geophys. Res. Lett.*, *21*, 2559–2562, 1994.

Kida, H., General circulation of air parcels and transport characteristics derived from a hemispheric GCM, Part 2, Very long-term motions of air parcels in the troposphere and stratosphere, *J. Meteorol. Soc. Jpn.*, *61*, 510–522, 1983.

McIntyre, M. E., Atmospheric dynamics: Some fundementals, with observational implications, in *The Use of EOS for Studies of Atmospheric Physics*, edited by J. C. Gille and G. Visconti, pp. 313–386, North-Holland, New York, 1992.

Minschwaner, K., A. E. Dessler, J. W. Elkins, C. M. Volk, D. W. Fahey, M. Lowenstein, J. R. Podolske, A. E. Roche, and K. R. Chan, The bulk properties of isentropic mixing into the tropics in the lower stratosphere, *J. Geophys. Res.*, *101*, 9433–9439, 1996.

Mote, P. W., K. H. Rosenlof, J. R. Holton, R. S. Harwood, and J. W. Waters, Seasonal variations of water vapor in the tropical lower stratosphere, *Geophys. Res. Lett.*, *22*, 1093–1096, 1995.

Mote, P. W., K. H. Rosenlof, M. E. McIntyre, E. S. Carr, J. C. Gille, J. R. Holton, J. S. Kinnersley, H. C. Pumphrey, J. M. Russell, and J. W. Waters, An atmospheric tape recorder: the imprint of tropical tropopause temperatures on stratospheric water vapor, *J. Geophys. Res.*, *101*, 3989–4006, 1996.

Murphy, M. M., D. M. Fahey, M. H. Proffitt, S. C. Liu, K. R. Chan, C. S. Eubank, S. R. Kawa, and K. K. Kelly, Reactive nitrogen and its correlation with ozone in the lower stratosphere and upper troposphere, *J. Geophys. Res.*, *98*, 8751–8773, 1993.

Oram, D. E., C. E. Reeves, S. A. Penkett, and P. J. Fraser,

Oram, D. E., C. E. Reeves, S. A. Penkett, and P. J. Fraser, Measurements of HCFC-142b and HCFC-141b in the Cape Grim air archive: 1978-1993, *Geophys. Res. Lett.*, *22*, 2741–2744, 1995.

Plumb, R. A., A tropical pipe model of stratospheric transport, *J. Geophys. Res.*, *101*, 3957–3972, 1996.

Plumb, R. A., and M. K. W. Ko, Interrelationships between mixing ratios of long-lived stratospheric constituents, *J. Geophys. Res.*, *97*, 10,145–10,156, 1992.

Plumb, R. A., and D. D. McConalogue, On the meridional structure of long-lived tropospheric constituents, *J. Geophys. Res.*, *93*, 15,897–15,913, 1988.

Pollock, W. A., L. E. Heidt, R. A. Lueb, J. F. Vedder, M. J. Mills, and S. Solomon, On the age of stratospheric air and ozone depletion potentials in the polar regions, *J. Geophys. Res.*, *97*, 12,993–12,999, 1992.

Prather, M. J., Numerical advection by conservation of second-order moments, *J. Geophys. Res.*, *91*, 6671–6681, 1986.

Prather, M. J., M. B. McElroy, S. C. Wofsy, G. Russell, and D. Rind, Chemistry of the global troposphere: Fluorocarbons as tracers of air motion, *J. Geophys. Res.*, *92*, 6579–6613, 1987.

Rasch, P. J., and D. L. Williamson, On shape-preserving interpolation and semi-Lagrangian transport, *SIAM J. Sci. Stat. Comput.*, *11*, 656–687, 1990.

Rasch, P. J., X. Tie, B. A. Boville, and D. L. Williamson, A three-dimensional transport model for the middle atmosphere, *J. Geophys. Res.*, *99*, 999–1017, 1994.

Rind, D., R. Suozzo, N. K. Balachandran, A. Lacis, and G. Russell, The GISS global climate/middle atmosphere model, I, Model structure and climatology, *J. Atmos. Sci.*, *45*, 329–370, 1988.

Rinsland, C. P., M. R. Gunson, M. C. Abrams, L. L. Lowes, R. Zander, and E. Mahieu, ATMOS/ATLAS 1 measurements of sulfer hexafluoride $SF_6$ in the lower stratosphere and upper troposphere, *J. Geophys. Res.*, *98*, 20,491–20,494, 1993.

Rosenlof, K. H., Seasonal cycle of the residual mean circulation in the stratosphere, *J. Geophys. Res.*, *100*, 5173–5191, 1995.

Schmidt, U., and A. Khedim, In situ measurements of carbon dioxide in the winter arctic vortex and at midlatitudes: An indicator of the age of stratospheric air, *Geophys. Res. Lett.*, *18*, 763–766, 1991.

Trepte, C. R., and M. H. Hitchman, Tropical stratospheric circulation deduced from satellite aerosol data, *Nature*, *355*, 626–628, 1992.

Volk, C. M., J. W. Elkins, D. W. Fahey, R. J. Salawitch, G. S. Dutton, J. M. Gilligan, M. H. Proffitt, M. Lowenstein, and P. R. Podolske, In-situ measurements constraining exchange between the tropics and middle latitudes in the lower stratosphere, *Science*, *272*, 1763–1768, 1996.

Weinstock, E. M., E. J. Hintsa, A. E. Dessler, and J. G. Anderson, Measurements of water vapor in the tropical lower stratosphere during the CEPEX campaign: Results and interpretation, *Geophys. Res. Lett.*, *22*, 3231–3234, 1995.

Williamson, D. L., and P. J. Rasch, Two-dimensional semi-Lagrangian transport with shape preserving interpolation, *Mon. Weather Rev.*, *117*, 102–129, 1989.

---

T. M. Hall and D. W. Waugh, Cooperative Research Centre for Southern Hemisphere Meteorology, Monash University, Building 70, Wellington Rd., Clayton VIC 3168, Australia. (email:hall@vortex.shm.monash.edu.au; waugh@vortex.shm.monash.edu.au)

(Received May 9, 1996; revised November 17, 1996; accepted November 19, 1996.)